Rapid Communications

Universal conductance fluctuations and direct observation of crossover of symmetry classes in topological insulators

Saurav Islam,[1,*] Semonti Bhattacharyya,[1,2] Hariharan Nhalil,[1] Suja Elizabeth,[1] and Arindam Ghosh[1,3]
[1]*Department of Physics, Indian Institute of Science, Bangalore 560012, India*
[2]*School of Physics and Astronomy, Monash University, Victoria 3800, Australia*
[3]*Center for Nanoscience and Engineering, Indian Institute of Science, Bangalore 560012, India*

(Received 4 May 2018; published 28 June 2018)

A key feature of topological insulators (TIs) is symplectic symmetry of the Hamiltonian which changes to unitary when time-reversal symmetry is lifted and a topological phase transition occurs. However, such a crossover has yet to be explicitly observed by directly probing the symmetry class of the Hamiltonian. In this Rapid Communication, we have probed the symmetry class of topological insulators by measuring the mesoscopic conductance fluctuations in the TI $Bi_{1.6}Sb_{0.4}Te_2Se$, which shows an exact factor of 2 reduction on application of a magnetic field due to a crossover from symplectic to unitary symmetry classes. The reduction provides an unambiguous proof that the fluctuations arise from the universal conductance fluctuations (UCFs), due to quantum interference, and persists from $T \sim 22$ mK to 4.2 K. We have also compared the phase breaking length l_ϕ extracted from both magnetoconductance and UCFs which agree well within a factor of 2 in the entire temperature and gate voltage range. Our experiment confirms UCF as the major source of fluctuations in mesoscopic disordered topological insulators, and the intrinsic preservation of time-reversal symmetry in these systems.

DOI: 10.1103/PhysRevB.97.241412

Topological insulators (TIs) [1–4] at zero magnetic field are time-reversal invariant systems characterized by surface states with a linear band structure. The Hamiltonian for such surface states is described by $H = \hbar v_F \vec{\sigma} \cdot \vec{k}$, which belongs to the AII/symplectic universality class, where v_F, $\vec{\sigma}$, and $\vec{k}$ are the Fermi velocity, spin matrices, and momentum, respectively. This is also known as the Anderson universality class for non-relativistic particles in the presence of a random spin-orbit coupling where time-reversal symmetry (TRS) is preserved [5]. The addition of an external magnetic field or ferromagnetic impurities introduces a Zeeman/orbital term in the Hamiltonian and breaks the TRS, which results in a topological to trivial phase transition in the bulk states and manifests as a gap opening in the linear surface states [3]. In terms of random matrix theory, this crossover at the surface states is well described by a crossover from AII/symplectic to A/unitary class in the system. Experimentally, the sensitivity of transport to magnetic impurities [6,7] or the saturation of the phase breaking length at low temperatures are directly connected to the TRS in TI systems [8,9]. This makes an explicit demonstration of the symplectic to unitary crossover an important task, which, however, has not yet been achieved.

One direct method to probe such a crossover of symmetry classes is universal conductance fluctuations (UCFs) [10–12], which are observed in mesoscopic devices, when the length of the sample L becomes comparable to l_ϕ, the phase breaking length. UCF is an effect which results from the quantum interference of all possible electron paths traversed between two points in a sample, making the electrical conduction sensitive to the Fermi energy, magnetic field, and impurity configuration. These fluctuations are independent of specific material properties or geometry, and are determined by the physical symmetries of the Hamiltonian. Within the framework of random matrix theory, the magnitude of UCF is proportional to [12]

$$\langle \delta G^2 \rangle \propto \left(\frac{e^2}{h}\right)^2 \frac{ks^2}{\beta}. \tag{1}$$

Here, β, s, and k are the Wigner-Dyson parameter, Kramer's degeneracy, and the number of independent eigenmodes of the Hamiltonian, respectively (Table I). This UCF-based technique has been previously used as an experimental probe in mesoscopic samples of graphene [13,14], where a factor of 4 reduction was observed in the magnitude as a function of number density due to a crossover from symplectic to orthogonal classes [15]. Similar reductions in the magnitude of the conductance fluctuations with magnetic field were observed in metal films [16–19], metallic single crystals of silicon [20], and also in δ-doped silicon-phosphorus systems [21,22]. Though a symmetry class crossover in TIs has been induced by the addition of ferromagnetic impurities and inferred from weak antilocalization [23], a more direct observation of the symmetry class and its crossover on breaking TRS, which does not require any addition of impurity, remains experimentally elusive. In this Rapid Communication, we present results of conductance fluctuation measurements in the topological insulator $Bi_{1.6}Sb_{0.4}Te_2Se$ on an atomically thin hexagonal boron nitride (hBN) substrate which shows a factor of 2 reduction on application of a magnetic field, thereby suggesting that the fluctuations indeed arise from UCF and the reduction is driven by a crossover from symplectic to unitary symmetry class. We have also extracted the phase breaking length from

*isaurav@iisc.ac.in

TABLE I. Values of symmetry parameters for the two classes relevant for TIs.

Ensemble	TRS	k	s	β	H_{ij}	$\langle \delta G^2 \rangle \propto (\frac{e^2}{h})^2 \frac{ks^2}{\beta}$
Symplectic	Yes	1	2	4	Real quaternion	1
Unitary	No	1	1	2	Complex	0.5

both magnetoconductance (l_ϕ^{MR}) and universal conductance fluctuations (l_ϕ^{UCF}) and found a close agreement.

The devices studied in this Rapid Communication were fabricated from an 11-nm-thick topological insulator $Bi_{1.6}Sb_{0.4}Te_2Se$ [24] exfoliated on a SiO_2/Si wafer and then transferred onto a 14-nm hBN substrate. The heterostructure was then finally transferred onto a heavily doped SiO_2/Si substrate with the 285-nm-thick SiO_2 acting as a back gate dielectric, using a home-made transfer technique. hBN was used to reduce the effect of dangling bonds and charged traps of the SiO_2 substrate on the electrical transport in the TI channel [25,26]. The quaternary alloy $Bi_{1.6}Sb_{0.4}Te_2Se$ offers a reduced bulk number density due to compensation doping resulting in an enhanced surface transport [24]. The contact pads were defined by standard electron-beam lithography followed by metallization using 5/40 nm Cr/Au [Fig. 1(a)]. The sample was coated with a layer of poly(methylmethacrylate) (PMMA) during the entire measurement cycle. All measurements from 22 mK to 4.2 K were done in a dilution refrigerator. Resistivity measurements were performed using a low-frequency ac four-probe technique with a carrier frequency of 18 Hz. The excitation current was 0.1 nA for most of the measurements to reduce the effect of Joule heating, except at 4.2 K, when it was increased to 1 nA. The resistance (R) vs gate voltage (V_G) is shown in Fig. 1(b), where a maximum in the resistance at $V_G \approx -38$ V at 5.5 K represents the Dirac point. The number density calculated at $V_G = 0$ V using $n = \frac{C_S(V_G - V_D)}{e}$ is -2.7×10^{16} m^{-2}. Here, C_S is the series capacitance of SiO_2 and hBN layers. Figure 1(c) shows a weak-antilocalization phenomenon characterized by a cusp in the quantum correction to conductivity $\triangle\sigma$ at $B = 0$ T [23,27–29]. Spin momentum locking in TI leads to an additional π Berry phase between the backscattered, time-reversed path of the carriers, leading to negative magnetoconductance, a signature of the symplectic phase. The magnetoconductance data can be fitted with the Hikami-Larkin-Nagaoka (HLN) equation for diffusive metals with high spin-orbit coupling ($\tau_\phi \gg \tau_{\mathrm{so}}, \tau_e$) [30,31],

$$\triangle\sigma = -\alpha \frac{e^2}{\pi h}\left[\psi\left(\frac{1}{2} + \frac{B_\phi}{B}\right) - \ln\left(\frac{B_\phi}{B}\right)\right], \qquad (2)$$

where τ_ϕ, τ_{so}, and τ_e are the phase coherence time, spin-orbit scattering time, and elastic scattering time, respectively, ψ is the digamma function, and B_ϕ is the phase breaking field. Here, α and B_ϕ are the fitting parameters. The phase coherence length (l_ϕ^{MR}) can be extracted using $l_\phi^{\mathrm{MR}} = \sqrt{\hbar/4eB_\phi}$. The value of α gives an estimate of the number of independent conducting channels in the sample. $\alpha = 0.5$ indicates a single transport channel whereas a value of 1 indicates two independent channels contributing to magnetotransport. In our case, the value of α at $T = 22$ mK [inset of Fig. 1(c)] varies from 0.8 near the Dirac point ($V_G = -60$ V) and gradually reduces to a value of around 0.6 for more positive gate voltages. This probably indicates that as the Fermi energy is tuned away from the charge neutrality point, the bulk carriers start contributing to transport, resulting in a reduction in the value of α, signifying the coupling of bulk and surface transport [8]. At maximum magnetic field, the classical contribution can be estimated using $\sigma_{\mathrm{CL}} = -\frac{\sigma_D^3}{n^2e^2}B^2 = 8 \times 10^{-4}\frac{e^2}{h}$, where $\sigma_D = 2.84 \times 10^{-4}$ s^{-1} is the Drude conductivity and $n = 8.5 \times 10^{16}$ m^{-2} at $V_G = 60$ V, which is negligible compared to the contribution from quantum interference.

The magnitude of conductance fluctuations $\langle \delta G^2 \rangle$ is evaluated using a method similar to Refs. [15,33] by varying the Fermi energy with the back gate voltage in steps of 5 mV over a small window of 4 V so that statistically meaningful data (about 800 realizations) are recorded, without changing the conductance appreciably in a two-terminal configuration for each transverse magnetic field. $\langle \delta G^2 \rangle$ is extracted from R-V_G by fitting the data with a smooth polynomial curve [15,33]. The variance of the residual of the fit gives the value of $\langle \delta R^2 \rangle$ and the mean value corresponds to $\langle R \rangle$. $\langle \delta G^2 \rangle$ is then obtained using the relation $\langle \delta G^2 \rangle = \langle \delta R^2 \rangle / \langle R \rangle^4$.

Figure 2(a) shows typical R-V_G sweeps at four different temperatures for the device, where the fluctuations decrease with T, a hallmark of UCF. The run-to-run reproducibility as a function of V_G in Fig. 2(b) further confirms the aperiodic yet reproducible nature of the fluctuations. The V_G dependence of $\langle \delta G^2 \rangle$ is shown in Fig. 2(c). The magnitude of $\langle \delta G^2 \rangle$ shows an increase as the Fermi energy is tuned away from the electron-hole puddle-dominated regime towards higher number densities. Such behavior is a unique signature of Dirac

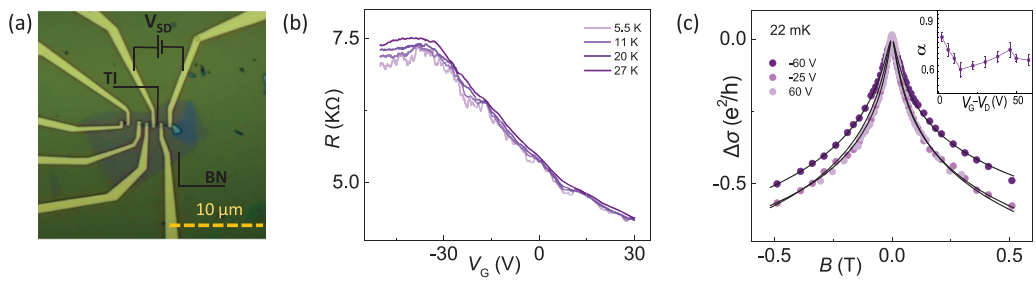

FIG. 1. Basic characteristics of a TI field effect transistor (FET). (a) Optical micrograph of a typical TI on a BN FET device. (b) R-V_G of the device at different temperatures. (c) Magnetoconductance at three different gate voltages at $T = 22$ mK. The solid lines are fits to the data according to Eq. (2) [the inset shows α extracted from the fits using Eq. (2)].

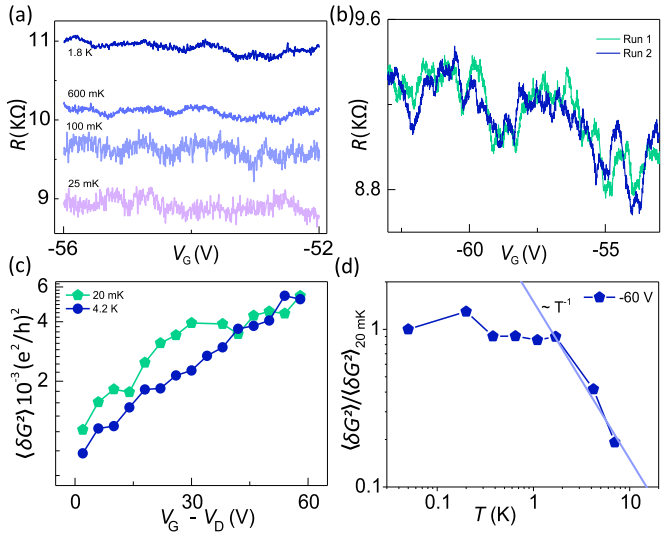

FIG. 2. Features of conductance fluctuations. (a) R-V_G in a small gate voltage window of 4 V for four different temperatures used to calculate $\langle\delta G^2\rangle$ by using a smooth polynomial fit. The curves have been offset for clarity. (b) R-V_G for two different runs showing the reproducibility of conductance fluctuations arising due to quantum interference. (c) Magnitude of conductance fluctuations as a function of gate voltage showing a monotonic increase away from the Dirac point. (d) T dependence of $\langle\delta G^2\rangle$ normalized by the magnitude at 20 mK showing a gradual decrease with increasing T, a characteristic feature of UCF. The solid line shows $\langle\delta G^2\rangle \sim 1/T$ for $T > 2$ K.

fermionic systems such as TI surface states, where the disorder potential due to charged impurities is long range in nature [15,34]. At more positive gate voltages, the values of $\langle\delta G^2\rangle$ at $T = 20$ mK and 4.2 K are similar. This may be due to an increased contribution of scattering due to bulk defects, which are the dominant source of noise in TIs [35–39]. The temperature dependence of conductance fluctuations [Fig. 2(d)] shows an increase as T is reduced to 2 K, below which it saturates. The saturation of $\langle\delta G\rangle^2$ at $T < 2$ K can be due to the saturation of l_ϕ. Such saturation has been previously seen in various systems and can arise due to the presence of magnetic impurities in the system [40] or when the spin-orbit length becomes comparable to the phase breaking length [41]. For $T > 2$ K, the magnitude of $\langle\delta G^2\rangle$ decreases with increasing T as $\langle\delta G^2\rangle \propto 1/T$, which can be explained from the dependence of $\langle\delta G^2\rangle$ on l_ϕ and the number of active fluctuators (n_s). For $T \to 0$, the UCF magnitude $\langle\delta G^2\rangle^{\frac{1}{2}} \to e^2/h$, while at finite temperatures [11,18,21],

$$\langle\delta G^2\rangle \simeq \left(\frac{e^2}{h}\right)^2 \alpha(k_F\delta r)\frac{1}{k_F l}\frac{L_y}{L_x^3} n_s(T) l_\phi^4, \tag{3}$$

where k_F, l, L_x, and L_y are the Fermi wave vector, mean free path, and sample dimensions in the x and y directions, respectively. $\alpha(x)$ represents the change of the phase of the electron wave function due to scattering by a moving impurity at a distance δr. Assuming electron-electron interaction-mediated dephasing, $l_\phi^2 \propto 1/T$ and $n_s(T) \propto T$ [11,18,21,42], we have $\langle\delta G^2\rangle \propto l_\phi^4 n_s(T) \propto 1/T$ [Fig. 2(d)], as observed at $T > 2$ K.

In order to (a) conclusively establish the role of UCF, and (b) investigate the crossover in the symmetry class directly, we have measured $\langle\delta G^2\rangle$ as a function of a perpendicular magnetic field ($B_\perp$) at fixed V_G. The magnitude of the conductance fluctuations is plotted as $v(B_\perp,T) = N_G(B_\perp)/N_G(B_\perp = 0)$, where $N_G = \langle\delta G^2\rangle/\langle G^2\rangle$ is the normalized variance. As a function of increasing $B_\perp$, as shown in Figs. 3(a) and 3(b) at $T = 22$ mK and $T = 4.2$ K, we observe a clear factor of 2 reduction in the UCF magnitude at -60 and -25 V, whereas at 60 V, the reduction significantly reduced. For gate voltages closer to the Dirac point (-60 and -25 V), the reduction occurs for $B_\perp \sim 0.01$–0.1 T, which is similar to the field scales for the quantum interference effect (B_ϕ) reported for TIs [8,43,44]. Since $B_\phi \sim \hbar/4el_\phi^2$, the increase in field scales with T can be readily attributed to the decrease in l_ϕ with increasing T. Although $l_\phi \propto T^{-1/2}$ as expected from electron-electron scattering would lead to a much larger change in B_ϕ in the experimental temperature range, we believe a saturation in l_ϕ [40,41] limits the decrease in B_ϕ at low temperatures. The absence of a factor of 2 reduction at high positive voltages is unlikely because of the opening of a gap in the surface states due to the magnetic field, since the reduction is independent of T scales that are either large ($K_BT \sim 0.362$ meV at 4.2 K) or very small ($K_BT \sim 0.00172$ meV at $T = 20$ mK) compared to the Zeeman energy scale ($\triangle E = g\mu_B B = 0.156$ meV at $B = 100$ mT), where $g = 27$ is the Landé g-factor and μ_B is the Bohr magneton [45]. The absence of the reduction by a factor of 2 can be due to additional noise contributions in the system. As E_F is tuned towards the bulk bands, trapping-detrapping processes from the charged impurities in the bulk, which are independent of $B_\perp$, and are known to be the dominant source of noise in TIs, increase [35–39], which diminishes the factor of 2 reduction.

To capture the nature of the crossover of the magnitude of the conductance fluctuations with B, as well as a quantitative evaluation of the crossover field scale, we have fitted the normalized magnitude with the expression [21,46,47]

$$\begin{aligned} v(B,T) &= \frac{1}{2} + \frac{1}{b^2}\sum_{n=0}^{\infty}\frac{1}{\left[\left(n+\frac{1}{2}\right)+\frac{1}{b}\right]^3} \\ &= \frac{1}{2} - \Psi''\frac{1}{2b^2}\left(\frac{1}{2}+\frac{1}{b}\right). \end{aligned} \tag{4}$$

Here, $b = 8\pi B(l_\phi)^2/(h/e)$, Ψ'' is the double derivative of the digamma function, and l_ϕ is the fitting parameter. The solid lines in Fig. 3 are fits according to Eq. (4), which capture well the variation of the magnitude of the conductance fluctuations with $B_\perp$, especially at gate voltage values close to the Dirac point. The corresponding l_ϕ, extracted from fitted values of b, are plotted in Fig. 4 (solid circles). At $V_G = 60$ V, the overall reduction allows us to estimate ≈28% of the observed magnitude of the conductance fluctuations to arise from UCF at $T = 20$ mK [Fig. 3(a)], but it becomes negligibly small at higher T [Fig. 3(b)].

Finally, we have evaluated the V_G dependence of l_ϕ from three different methods: (a) $\langle\delta G^2\rangle$ magnitude, (b) $B_\perp$ dependence of conductance fluctuations, and (c)

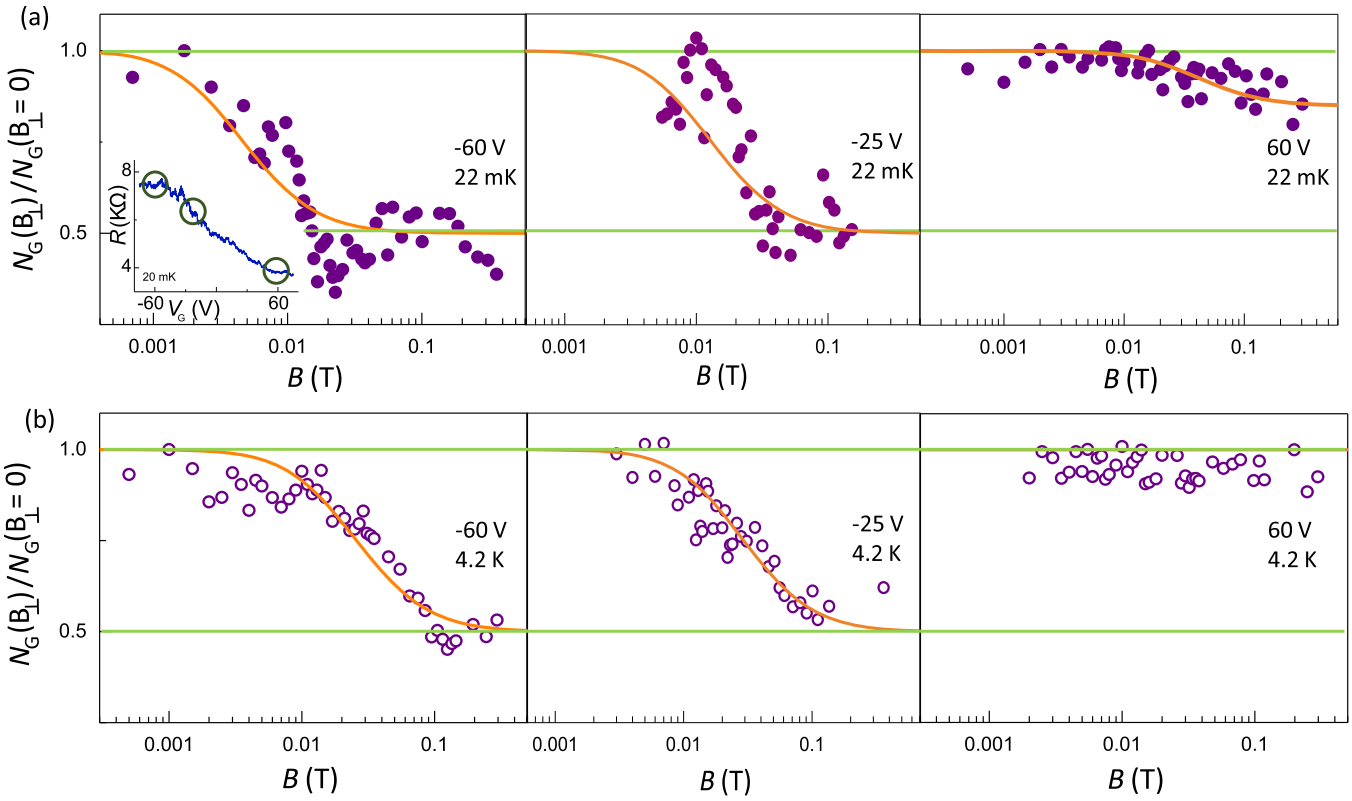

FIG. 3. Magnetic field dependence of normalized UCF magnitude. (a) $v(B_\perp,T) = N_G(B_\perp)/N_G(B_\perp = 0)$ for three different gate voltages (−60, −25, and 60 V) for 22 mK clearly exhibiting a factor of 2 reduction which diminishes as the Fermi energy is tuned towards the bulk. The solid lines indicate fits to the data using Eq. (4). The normalized conductance fluctuation data for 60 V at $T = 20$ mK has been fitted using the crossover function $v'(B,T)$ (as shown in the Supplemental Material [32]). The inset in (a) shows R vs V_G at $T = 20$ mK. The circled regions indicate windows where UCF was measured. (b) Normalized UCF magnitude at three gate voltage −60, −25, and 60 V at 4.2 K. The solid lines indicate fits to the data using Eq. (4).

magnetoconductance. We have, however, restricted the calculation between $V_G = -60$ and 0 V, where UCF is the dominant source of noise. l_ϕ, extracted directly from $\langle \delta G^2 \rangle$ at $B_\perp = 0$ T using the expression [5,48,49]

$$\langle \delta G^2 \rangle \simeq \frac{3}{\pi}\left(\frac{e^2}{h}\right)^2\left(\frac{l_\phi}{L}\right)^2, \tag{5}$$

is shown in Fig. 4 [$L = W$ (width) $= 2$ μm] (open circles), while $l_\phi^{\rm MR}$, extracted from magnetoconductance using Eq. (2), is shown in the inset of Fig. 4. We find that $l_\phi^{\rm MR}$ and $l_\phi^{\rm UCF}$ [obtained from both Eqs. (4) and (5)] are similar in magnitude within a factor of 2, rendering the validity to the factor of 2 reduction and the corresponding analysis. $l_\phi^{\rm MR}$ increases away from the Dirac point, similar to the trend of l_ϕ obtained from UCF (Fig. 4). Near the Dirac point, the system is highly inhomogeneous, with the presence of electron-hole puddles. As the gate voltage is tuned away from the charge neutrality point, the carrier concentration increases, leading to enhanced screening which suppresses dephasing due to electromagnetic fluctuations from inelastic scattering. This leads to a larger l_ϕ away from the Dirac point [50–55]. The factor of 2 difference in $l_\phi^{\rm MR}$ and $l_\phi^{\rm UCF}$ can arise because Eq. (5) is valid in the case of $l_\phi \ll L, L_T$ [5,49], where L_T is the thermal length. Moreover, τ_ϕ relevant for weak localization is related to the Nyquist dephasing rate [42], while for UCF τ_ϕ may be related to the inverse of the inelastic collision frequency, and may differ from each other by a logarithmic factor [16,21,56–59].

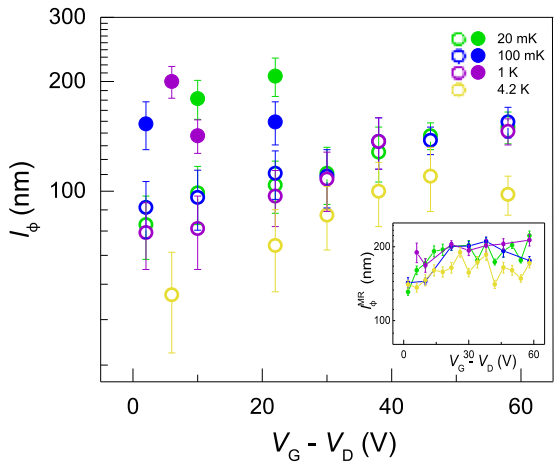

FIG. 4. Comparison of phase breaking length (l_ϕ) from different methods. l_ϕ extracted from UCF as a function of V_G for different T from magnetic field dependence using Eq. (4) (solid circles) and directly at $B_\perp = 0$ T using Eq. (5) (open circles). The inset shows $l_\phi^{\rm MR}$ extracted from magnetoconductance using Eq. (2) as a function of V_G for different T. l_ϕ obtained from three different methods agree well, within a factor of 2.

In conclusion, we have measured the Fermi-energy-dependent aperiodic and reproducible fluctuations in mesoscopic topological insulator systems. The magnetic field dependence of these fluctuations conclusively indicates that they arise from universal conductance fluctuations. Most importantly, a factor of 2 reduction in noise magnitude close to the Dirac point is observed, which provides an unambiguous proof that the time-reversal symmetry in disordered topological insulators is intrinsically maintained.

We thank Saquib Shamim for useful discussions. We acknowledge the Department of Science and Technology (DST), Government of India for funding.

[1] M. Z. Hasan and C. L. Kane, Rev. Mod. Phys. **82**, 3045 (2010).
[2] J. E. Moore, Nature (London) **464**, 194 (2010).
[3] B. A. Bernevig, T. L. Hughes, and S.-C. Zhang, Science **314**, 1757 (2006).
[4] M. König, S. Wiedmann, C. Brüne, A. Roth, H. Buhmann, L. W. Molenkamp, X.-L. Qi, and S.-C. Zhang, Science **318**, 766 (2007).
[5] P. Adroguer, D. Carpentier, J. Cayssol, and E. Orignac, New J. Phys. **14**, 103027 (2012).
[6] C.-Z. Chang, J. Zhang, X. Feng, J. Shen, Z. Zhang, M. Guo, K. Li, Y. Ou, P. Wei, L.-L. Wang, Z.-Q. Ji, Y. Feng, S. Ji, X. Chen, J. Jia, X. Dai, Z. Fang, S.-C. Zhang, K. He, Y. Wang, L. Lu, X.-C. Ma, and Q.-K. Xue, Science **340**, 167 (2013).
[7] L. Bao, W. Wang, N. Meyer, Y. Liu, C. Zhang, K. Wang, P. Ai, and F. Xiu, Sci. Rep. **3**, 2391 (2013).
[8] J. Liao, Y. Ou, H. Liu, K. He, X. Ma, Q.-K. Xue, and Y. Li, Nat. Commun. **8**, 16071 (2017).
[9] F. Pierre, A. B. Gougam, A. Anthore, H. Pothier, D. Esteve, and N. O. Birge, Phys. Rev. B **68**, 085413 (2003).
[10] P. A. Lee and A. D. Stone, Phys. Rev. Lett. **55**, 1622 (1985).
[11] S. Feng, P. A. Lee, and A. D. Stone, Phys. Rev. Lett. **56**, 1960 (1986).
[12] B. Altshuler and B. Shklovskii, Zh. Eksp. Teor. Fiz. **91**, 220 (1986).
[13] K. S. Novoselov, A. K. Geim, S. V. Morozov, D. Jiang, Y. Zhang, S. V. Dubonos, I. V. Grigorieva, and A. A. Firsov, Science **306**, 666 (2004).
[14] A. C. Neto, F. Guinea, N. M. Peres, K. S. Novoselov, and A. K. Geim, Rev. Mod. Phys. **81**, 109 (2009).
[15] A. N. Pal, V. Kochat, and A. Ghosh, Phys. Rev. Lett. **109**, 196601 (2012).
[16] P. McConville and N. O. Birge, Phys. Rev. B **47**, 16667 (1993).
[17] N. O. Birge, B. Golding, and W. H. Haemmerle, Phys. Rev. Lett. **62**, 195 (1989).
[18] N. O. Birge, B. Golding, and W. H. Haemmerle, Phys. Rev. B **42**, 2735 (1990).
[19] J. S. Moon, N. O. Birge, and B. Golding, Phys. Rev. B **53**, R4193 (1996).
[20] A. Ghosh and A. K. Raychaudhuri, Phys. Rev. Lett. **84**, 4681 (2000).
[21] S. Shamim, S. Mahapatra, G. Scappucci, W. Klesse, M. Simmons, and A. Ghosh, Sci. Rep. **7**, 46670 (2017).
[22] S. Shamim, S. Mahapatra, G. Scappucci, W. M. Klesse, M. Y. Simmons, and A. Ghosh, Phys. Rev. Lett. **112**, 236602 (2014).
[23] H.-T. He, G. Wang, T. Zhang, I.-K. Sou, G. K. L. Wong, J.-N. Wang, H.-Z. Lu, S.-Q. Shen, and F.-C. Zhang, Phys. Rev. Lett. **106**, 166805 (2011).
[24] A. A. Taskin, Z. Ren, S. Sasaki, K. Segawa, and Y. Ando, Phys. Rev. Lett. **107**, 016801 (2011).
[25] C. R. Dean, A. F. Young, I. Meric, C. Lee, L. Wang, S. Sorgenfrei, K. Watanabe, T. Taniguchi, P. Kim, K. L. Shepard *et al.*, Nat. Nanotechnol. **5**, 722 (2010).
[26] P. Karnatak, T. P. Sai, S. Goswami, S. Ghatak, S. Kaushal, and A. Ghosh, Nat. Commun. **7**, 13703 (2016).
[27] L. Zhang, M. Dolev, Q. I. Yang, R. H. Hammond, B. Zhou, A. Palevski, Y. Chen, and A. Kapitulnik, Phys. Rev. B **88**, 121103 (2013).
[28] Y. S. Kim, M. Brahlek, N. Bansal, E. Edrey, G. A. Kapilevich, K. Iida, M. Tanimura, Y. Horibe, S.-W. Cheong, and S. Oh, Phys. Rev. B **84**, 073109 (2011).
[29] N. Bansal, Y. S. Kim, M. Brahlek, E. Edrey, and S. Oh, Phys. Rev. Lett. **109**, 116804 (2012).
[30] S. Hikami, A. I. Larkin, and Y. Nagaoka, Prog. Theor. Phys. **63**, 707 (1980).
[31] L. Bao, L. He, N. Meyer, X. Kou, P. Zhang, Z.-G. Chen, A. V. Fedorov, J. Zou, T. M. Riedemann, T. A. Lograsso *et al.*, Sci. Rep. **2**, 726 (2012).
[32] See Supplemental Material at http://link.aps.org/supplemental/10.1103/PhysRevB.97.241412 for estimation of the magnitude of conductance fluctuations, fit of magnetic field dependence of conductance fluctuations, magnetoresistance fitting at 4.2 K, and α extracted from the HLN equation.
[33] R. V. Gorbachev, F. V. Tikhonenko, A. S. Mayorov, D. W. Horsell, and A. K. Savchenko, Phys. Rev. Lett. **98**, 176805 (2007).
[34] E. Rossi, J. H. Bardarson, M. S. Fuhrer, and S. Das Sarma, Phys. Rev. Lett. **109**, 096801 (2012).
[35] S. Bhattacharyya, M. Banerjee, H. Nhalil, S. Islam, C. Dasgupta, S. Elizabeth, and A. Ghosh, ACS Nano **9**, 12529 (2015).
[36] S. Bhattacharyya, A. Kandala, A. Richardella, S. Islam, N. Samarth, and A. Ghosh, Appl. Phys. Lett. **108**, 082101 (2016).
[37] S. Islam, S. Bhattacharyya, A. Kandala, A. Richardella, N. Samarth, and A. Ghosh, Appl. Phys. Lett. **111**, 062107 (2017).
[38] J. Pelz and J. Clarke, Phys. Rev. B **36**, 4479 (1987).
[39] S. Hershfield, Phys. Rev. B **37**, 8557 (1988).
[40] F. Schopfer, C. Bäuerle, W. Rabaud, and L. Saminadayar, Phys. Rev. Lett. **90**, 056801 (2003).
[41] Y. K. Fukai, S. Yamada, and H. Nakano, Appl. Phys. Lett. **56**, 2123 (1990).
[42] B. L. Altshuler, A. Aronov, and D. Khmelnitsky, J. Phys. C: Solid State Phys. **15**, 7367 (1982).
[43] S. Zhang, R. McDonald, A. Shekhter, Z. Bi, Y. Li, Q. Jia, and S. T. Picraux, Appl. Phys. Lett. **101**, 202403 (2012).
[44] Z. Li, Y. Meng, J. Pan, T. Chen, X. Hong, S. Li, X. Wang, F. Song, and B. Wang, APEX **7**, 065202 (2014).
[45] A. Wolos, S. Szyszko, A. Drabinska, M. Kaminska, S. Strzelecka, A. Hruban, A. Materna, M. Piersa, J. Borysiuk, K. Sobczak *et al.*, Phys. Rev. B **93**, 155114 (2016).

[46] A. D. Stone, Phys. Rev. B **39**, 10736 (1989).
[47] P. A. Lee, A. D. Stone, and H. Fukuyama, Phys. Rev. B **35**, 1039 (1987).
[48] C. Beenakker and H. van Houten, in *Solid State Physics*, Vol. 44 (Elsevier, Amsterdam, 1991), pp. 1–228.
[49] E. Akkermans and G. Montambaux, *Mesoscopic Physics of Electrons and Photons* (Cambridge University Press, Cambridge, UK, 2007).
[50] J. Tian, C. Chang, H. Cao, K. He, X. Ma, Q. Xue, and Y. P. Chen, Sci. Rep. **4**, 4859 (2014).
[51] S.-P. Chiu and J.-J. Lin, Phys. Rev. B **87**, 035122 (2013).
[52] J. Martin, N. Akerman, G. Ulbricht, T. Lohmann, J. H. Smet, K. von Klitzing, and A. Yacoby, Nat. Phys. **4**, 144 (2008).
[53] H. Steinberg, J.-B. Laloë, V. Fatemi, J. S. Moodera, and P. Jarillo-Herrero, Phys. Rev. B **84**, 233101 (2011).
[54] S. V. Morozov, K. S. Novoselov, M. I. Katsnelson, F. Schedin, L. A. Ponomarenko, D. Jiang, and A. K. Geim, Phys. Rev. Lett. **97**, 016801 (2006).
[55] D.-K. Ki, D. Jeong, J.-H. Choi, H.-J. Lee, and K.-S. Park, Phys. Rev. B **78**, 125409 (2008).
[56] Y. M. Blanter, Phys. Rev. B **54**, 12807 (1996).
[57] D. Hoadley, P. McConville, and N. O. Birge, Phys. Rev. B **60**, 5617 (1999).
[58] A. Trionfi, S. Lee, and D. Natelson, Phys. Rev. B **70**, 041304 (2004).
[59] V. Chandrasekhar, P. Santhanam, and D. E. Prober, Phys. Rev. B **44**, 11203 (1991).